

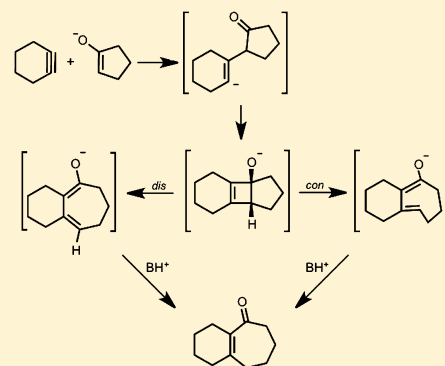
A Theoretical Study of Cyclohexyne Addition to Carbonyl–C_α Bonds: Allowed and Forbidden Electrocyclic and Nonpericyclic Ring-Openings of Strained Cyclobutenes

C. Avery Sader and K. N. Houk*

Department of Chemistry and Biochemistry, University of California, Los Angeles, California 90095-1569, United States

S Supporting Information

ABSTRACT: The mechanism of cyclohexyne insertion into a C(O)–C_α bond of cyclic ketones, explored experimentally by the Carreira group, has been investigated using density functional theory. B3LYP and M06–2X calculations were performed in both gas phase and THF (CPCM, UAKS radii). The reaction proceeds through a stepwise [2 + 2] cycloaddition of cyclohexyne to the enolate, followed by three disparate ring-opening possibilities of the cyclobutene alkoxide to give the product: (1) thermally allowed conrotatory electrocyclic ring-opening, (2) thermally forbidden disrotatory electrocyclic ring-opening, or (3) nonpericyclic C–C bond cleavage. Our computational results for the model alkoxide and potassium alkoxide systems show that the thermally allowed electrocyclic ring-opening pathway is favored by less than 1 kcal/mol. In more complex systems containing a potassium alkoxide (e–f), the barrier of the allowed conrotatory ring-opening is disfavored by 4–8 kcal/mol. This suggests that the thermodynamically more stable disrotatory product can be formed directly through a “forbidden” pathway. Analysis of geometrical parameters and atomic charges throughout the ring-opening pathways provides evidence for a nonpericyclic C–C bond cleavage, rather than a thermally forbidden disrotatory ring-opening. A true forbidden disrotatory ring-opening transition structure was computed for the cyclobutene alcohol; however, it was 19 kcal/mol higher in energy than the allowed conrotatory transition structure. An alternate mechanism in which the disrotatory product forms via isomerization of the conrotatory product was also explored for the alkoxide and potassium alkoxide systems.



INTRODUCTION

Arynes and cycloalkynes are potentially useful building blocks in organic synthesis.^{1–3} Stoltz and Tambar have reported a mild direct aryne insertion into C–C bonds.¹ They obtained an unexpected C–C addition product (boxed; Scheme 1) in comparable yield with the expected product.

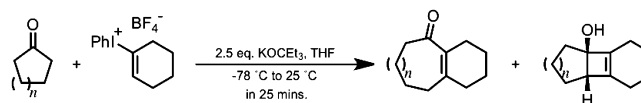
Scheme 1. Acyl-Alkylation of Benzyne into a β-Ketoester



Carreira and co-workers recently reported the formal addition of cyclohexyne to C–C bonds of cyclic ketones to yield medium-sized fused ring systems.² This process involves simultaneous formation of an enolate from a cyclic ketone and formation of cyclohexyne via base-induced elimination from an iodonium salt of cyclohexene. In some cases, a tricyclic product containing a cyclobutene ring is produced, suggesting the intermediacy of

this [2 + 2] cycloaddition product in formation of the cycloheptenone, as shown in Scheme 2.

Scheme 2. Cycloinsertion Reaction of Cyclohexyne into Cyclic Ketones



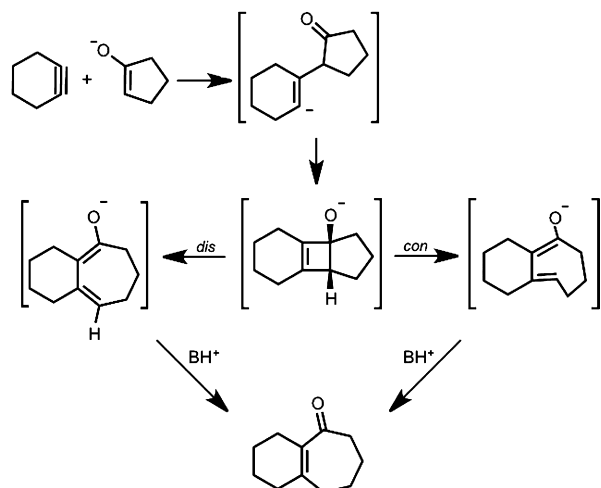
Carreira and Gampe have applied this reaction to the total synthesis of guanacastepenes,³ and a comprehensive review of their applications of this ring expansion reaction has recently been documented.⁴ Comandini and Brezinsky computationally explored the potential energy surface of a radical/ π -bond addition mechanism of *o*-benzyne to cyclopentadiene. One of the multiple pathways they studied involved the disrotatory electrocyclic ring-opening of a strained cyclobutene; however, it seems that the allowed conrotatory ring-opening was not considered.⁵ To determine the details of this cycloalkyne insertion mechanism, a computational study using density functional theory (DFT)

Received: February 12, 2012

Published: April 26, 2012

calculations was initiated. Of prime interest in this study was the nature of the electrocyclic ring-opening step (Scheme 3).

Scheme 3. Proposed Mechanism of Cycloinsertion Reaction



COMPUTATIONAL METHODS

Intermediate and transition state geometry optimizations were performed with Gaussian 09 using the hybrid functional B3LYP with the 6-31G(d) basis set or LANL2DZ for potassium.⁶ In addition, the anions were optimized with the diffuse 6-311++G(d,p) basis set. A stability check of the restricted wave function was performed to ensure that open-shell wave functions are not more stable.⁷ Analytical frequencies were calculated for each optimized structure using the corresponding level of theory. Single point energy calculations were performed with M06-2X/6-311++G(d,p) on B3LYP/6-31G(d) geometries and thermally corrected using the B3LYP/6-31G(d) vibrational data in order to report enthalpies. Such calculations have been shown to give improved thermodynamics for C–C bond forming reactions.⁸ All optimized saddle points were explored by intrinsic reaction coordinate (IRC)^{9,10} calculations, ensuring that they connect the appropriate reactants and products on the potential energy surface.

The effects of THF solvation on the reaction energetics were evaluated using the conductor-like polarizable continuum solvation model (CPCM).¹¹ The solute surface was defined by UAKS radii.¹²

RESULTS AND DISCUSSION

Reaction of Cyclohexyne and Cyclopentanone Enolate. The cycloaddition step was confirmed by our calculations to be stepwise, in accordance with the Woodward–Hoffmann rules. The energetics of cycloaddition are summarized in Figure 1.

Nucleophilic attack on cyclohexyne is the first step of the reaction and occurs without an activation barrier. Examples of nucleophilic additions to cycloalkynes without a barrier of activation have been reported elsewhere in the literature.¹³ The addition is exceedingly exothermic, forming 3a with a ΔH of -36 to -48 kcal/mol. Our calculations show that the alkyne (1) is distorted from linearity by 48° , which is in agreement with past theoretical studies of cyclohexyne using Hartree–Fock, DFT, or Møller–Plesset perturbation theory methods.^{14–16} The C–C and C–O bond lengths in cyclopentanone enolate (2a) are representative of enolate character. Figure 2 shows the geometries of cyclopentanone enolate nucleophilic addition to cyclohexyne optimized in the gas phase with B3LYP/6-31G(d) and B3LYP/6-311++G(d,p).

Ring closure of vinyl anion 3a to form cyclobutene alkoxide 5a has an activation barrier of only 2–5 kcal/mol and is

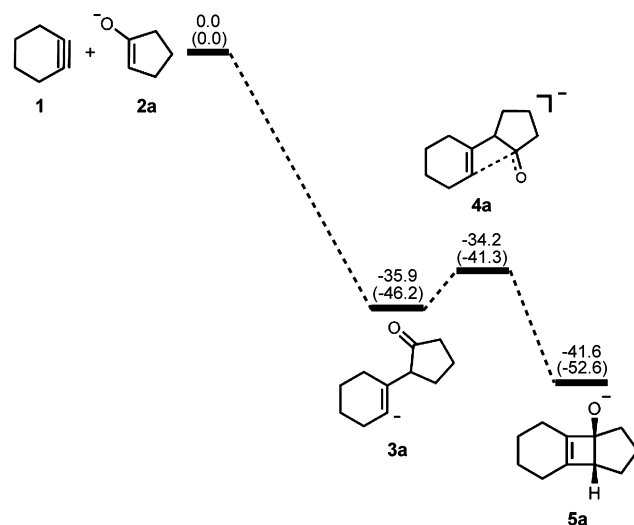


Figure 1. Stationary points on the energy surface for cycloaddition of cyclohexyne and cyclopentanone enolate. B3LYP/6-311++G(d,p) thermal energies, ΔH , with thermally corrected M06-2X/6-311++G(d,p)//B3LYP/6-31G(d) energies, ΔH , in parentheses, shown in kcal/mol.

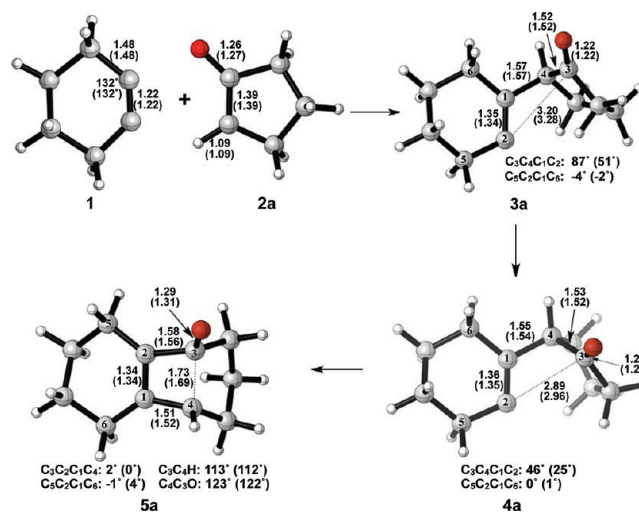


Figure 2. Optimized geometries of cyclohexyne insertion into cyclopentanone enolate. B3LYP/6-31G(d) selected bond distances (Å), angles, and dihedral angles with B3LYP/6-311++G(d,p) in parentheses are shown.

exothermic by only 6–7 kcal/mol. Structural deviations from normal cyclobutene geometries are immediately apparent in the bond lengths of 5a. A computational study by Houk and Rondan showed that donor substituents like alkoxide groups interact strongly with the C_3 – C_4 σ^* orbital in cyclobutene, thereby lowering the barrier to ring-opening.¹⁷ This hyperconjugative effect results in an increase of the C_3 – C_4 bond length as well as a decrease of the C_3 –O bond length relative to unsubstituted cyclobutene and is evident in the C_3 – C_4 bond length of 1.69 Å and the C_3 –O bond length of 1.31 Å.

Electrocyclic ring-opening of 5a is the next step in the pathway, and the energetics are summarized in Figure 3. The experimental enthalpy of activation for the electrocyclic ring-opening of cyclobutene is 32.5 ± 0.5 kcal/mol, and the reaction is exothermic by 10.8 kcal/mol.¹⁸ According to the Woodward–Hoffmann rules, cyclobutene undergoes a symmetry-allowed conrotatory ring-opening under thermal conditions. Numerous experimental and computational studies have

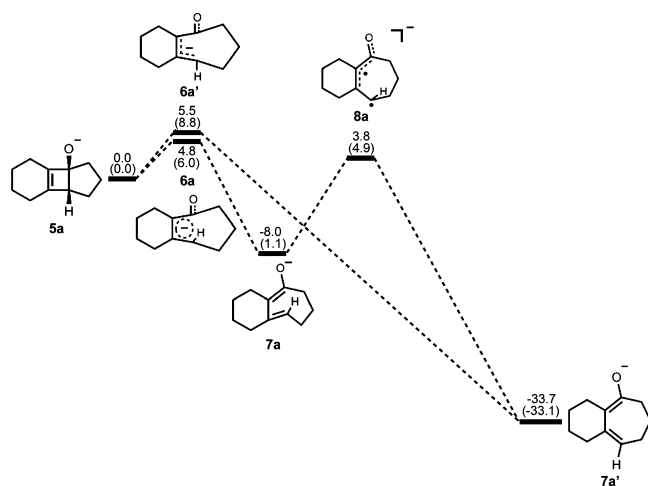


Figure 3. Stationary points on the energy surface for electrocyclic ring-opening and *cis*–*trans* isomerization. B3LYP/6-311++G(d,p) thermal energies, ΔH , with thermally corrected M06–2X/6-311++G(d,p)//B3LYP/6-31G(d) energies, ΔH , in parentheses, shown in kcal/mol.

confirmed this preference.^{17–21} Specifically, experiments by Brauman and Golden estimated that the allowed conrotatory process is 15.0 kcal/mol more favorable than the forbidden disrotatory process.²¹ The results of our computational study showed the enthalpy of activation for the allowed conrotatory electrocyclic ring-opening of **5a** is 4.8 (6.0) kcal/mol, and the reaction is exothermic by 8.0 kcal/mol by B3LYP but slightly endothermic by M06–2X. Nonpericyclic C–C bond cleavage gave an enthalpy of activation of 5.5 (8.0) kcal/mol and an exothermicity of 34 kcal/mol, only slightly higher than the allowed conrotatory pathway. We use the term “nonpericyclic” since there appears to be no cyclic delocalization, and this transition state appears to be different from pseudopericyclic transition states of electrocyclic reactions. The term “pseudopericyclic” was first used by Lemal to describe reactions that are characterized by the exchange of roles between orthogonal bonding and nonbonding atomic orbitals.²² Computational investigations have provided evidence that pseudopericyclic transition states are typically planar with no rotation of the terminal π -bonds. For instructive reviews of the subject, the reader is directed to articles of Kappe et al.,²³ Birney et al.,²⁴ and references therein. Isomerization of **7a** via **8a** forms the more stable product **7a'**. The difference between the enthalpies of reaction in the conrotatory and nonpericyclic cases is due to formation of a strained *cis,trans*-cycloheptadiene skeleton in the former and a relatively stable *cis,cis*-cycloheptadiene skeleton in the latter.

The optimized geometries of conrotatory and nonpericyclic ring-opening are shown in Figure 4. Previous work has shown that the skeleton of the conrotatory transition structure of cyclobutene is nonplanar ($\phi \approx 15^\circ$), while the disrotatory transition structure is planar.²⁵ It was also found that constraining planarity in the conrotatory transition structure reduces overlap between the σ orbital of the breaking bond and the π orbital present in cyclobutene. It was concluded that this reduction in stabilizing orbital overlap lowers the preference for the allowed conrotatory pathway. As seen in Figure 4, the $C_3C_2C_1C_4$ dihedral angle of the conrotatory transition structure is 5° , considerably more planar than the transition state of cyclobutene itself.

A number of investigations in the literature provide evidence that *cis*–*trans* isomerization can occur in similarly strained

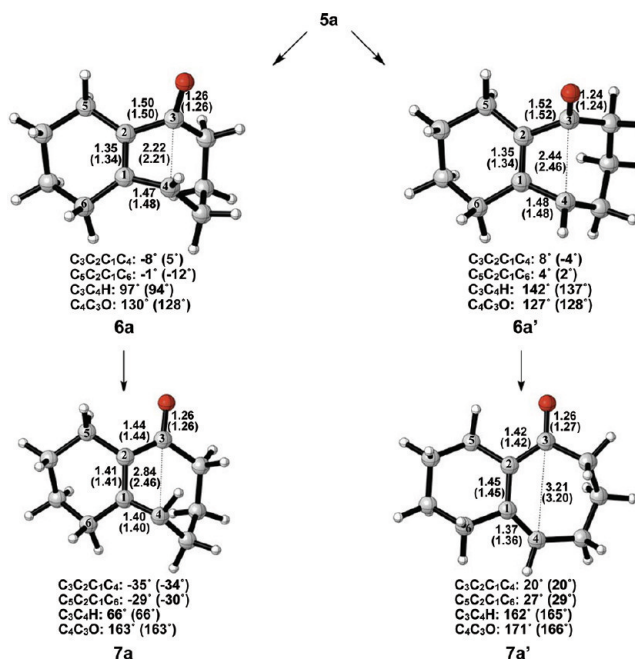


Figure 4. Optimized geometries of conrotatory (left) and nonpericyclic (right) ring-opening of cyclobutene alkoxide **5a**. B3LYP/6-31G(d) selected bond distances (Å) and dihedral angles, with B3LYP/6-311++G(d,p) in parentheses, are shown.

systems, directly connecting conrotatory products to disrotatory products on the potential energy surface.^{26–29} No such transition structure was found using spin-restricted B3LYP; however, use of broken symmetry, spin-unrestricted B3LYP successfully yielded structure **8a** (Figure 5). This result clearly

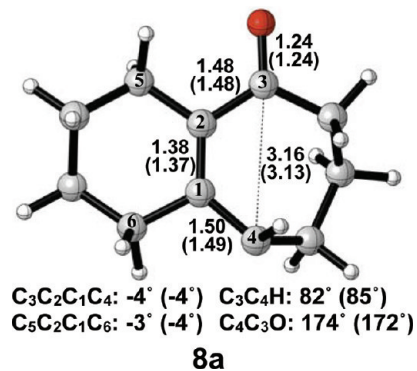


Figure 5. Optimized transition structure of *cis*–*trans* isomerization of alkoxide intermediate **7a** to **7a'**. B3LYP/6-31G(d) selected bond distances (Å), angles, and dihedral angles, with B3LYP/6-311++G(d,p) in parentheses, are shown.

indicates diradical character, which is known to exist in transition structures of π -bond rotation. Elongated C_1 – C_4 and C_2 – C_3 bond lengths relative to **6a** indicate more single-bond character and provide further evidence for the diradical nature of **8a**. The decreased C_1 – C_2 bond length also supports this idea. It is worthwhile to note that the C_3 – C_4 distance has increased almost to its final value of 3.20 Å as seen in **7a'**, while a comparatively small amount of outward rotation of C_4 –H has occurred. The enthalpy of activation for *cis*–*trans* isomerization was calculated as 12 kcal/mol.

Reaction of Cyclohexyne and Cyclopentanone Potassium Enolate in THF. An equivalent analysis of the reaction mechanism and energetics was performed with cyclohexyne and cyclopentanone potassium enolate. While potassium will be solvated in solution, this model provides a picture of the extreme effect of ion pairing on the reaction pathway. The energetics of cycloaddition are summarized in Figure 6.

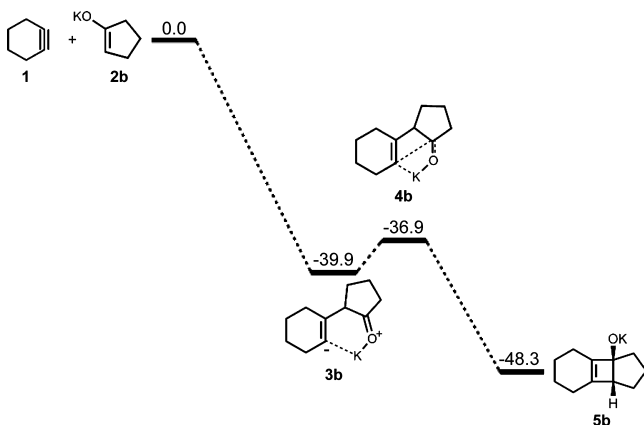


Figure 6. Stationary points on the energy surface for cycloaddition of cyclohexyne and cyclopentanone potassium enolate. B3LYP/6-31G(d) thermal energies, ΔH , shown in kcal/mol.

The addition yields an intermediate with a ΔH of -40 kcal/mol. For ring closure, an activation barrier of 3 kcal/mol was computed, and the reaction is exothermic by 8 kcal/mol.

Figure 7 shows the geometries of cyclohexyne insertion into cyclopentanone potassium enolate optimized in THF with

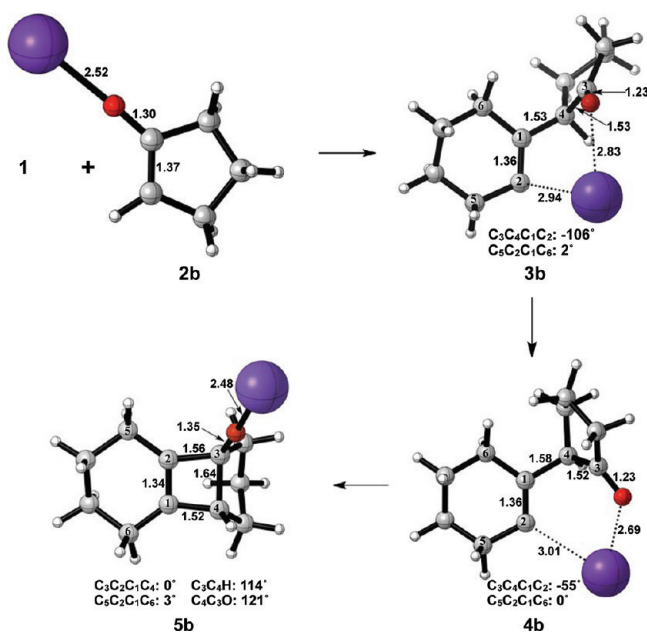


Figure 7. Optimized geometries in the cyclohexyne insertion into cyclopentanone potassium enolate. B3LYP/6-31G(d) selected bond distances (Å), angles, and dihedral angles are shown. LANL2DZ was used for potassium.

B3LYP/6-31G(d), using LANL2DZ for potassium. As shown by the bond distances in **3b** and **4b**, the potassium ion is stabilizing the development of charge on both the oxygen of the

cyclopentanone enolate and C2 of cyclohexyne. A C_3-C_4 bond length of 1.64 Å and a C_3-O bond length of 1.35 Å in **5b** both indicate less donation of electron density of oxygen into the σ^* orbital of C_3-C_4 when compared to the bare enolate. As a direct consequence, the barrier to electrocyclic ring-opening of **5b** is 10 kcal/mol greater than the electrocyclic ring-opening of **5a** (Figures 3 and 8).

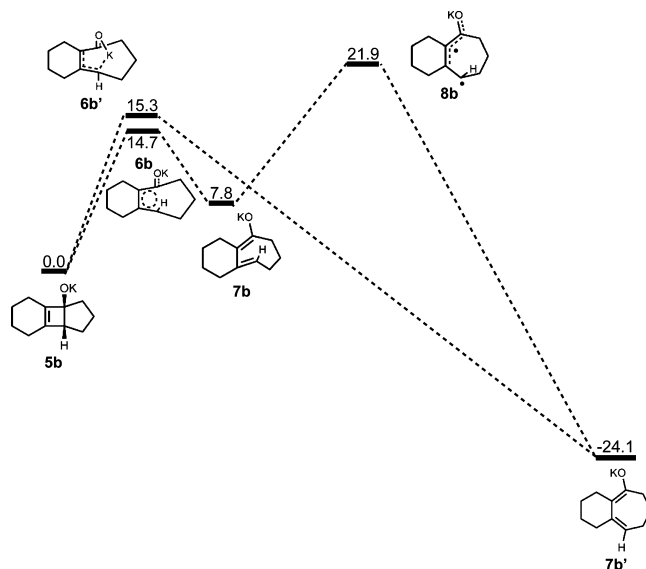


Figure 8. Stationary points on the energy surface for electrocyclic ring-opening and *cis-trans* isomerization. B3LYP/6-31G(d) thermal energies, ΔH , shown in kcal/mol.

The electrocyclic ring-opening step favors the allowed conrotatory process by about 1 kcal/mol; however, unlike the case of cyclopentanone enolate, the barrier of *cis-trans* isomerization is greater than both the barrier for subsequent ring closing (reversion) and the barrier for nonpericyclic ring-opening. The energetics of ring-opening are summarized in Figure 8. Optimized geometries of conrotatory and nonpericyclic ring-opening are shown in Figure 9. The $C_3C_2C_1C_4$ dihedral angles of the conrotatory and nonpericyclic transition structures are 18° and -4° , respectively, which closely resemble 19° and $\sim 0^\circ$,²⁵ those of the ring-opening transition structures of cyclobutene itself. There is an apparent interaction between the potassium and C4 in the nonpericyclic transition structure (**6b'**), but the preference for the allowed conrotatory ring-opening is less than 1 kcal/mol, about the same as in the free alkoxide. The reaction leading to the conrotatory product **7b** is endothermic by 8 kcal/mol. As in the case where potassium is absent, the large thermodynamic difference between **7b** and **7b'** is due to the presence of a trans double bond in the 7-membered conrotatory product.

A transition structure connecting the *cis/trans* product **7b** to the *cis/cis* product **7b'** is shown in Figure 10. Like the free alkoxide, *cis-trans* isomerization by direct π -bond rotation occurs here, necessitating the use of open-shell DFT to locate this transition structure. The C_3-C_4 bond elongates from 1.38 to 1.50 Å, and the C_2-C_3 bond elongates from 1.42 to 1.46 Å. The C_3-C_4 bond length of 3.15 Å and $C_3C_2C_1C_4$ dihedral angle of -4° in **8b** are both essentially the final values observed in **7b'**. Interestingly, the C_4C_3O bond angle has increased to 175° , more than that seen in the disrotatory product, while the

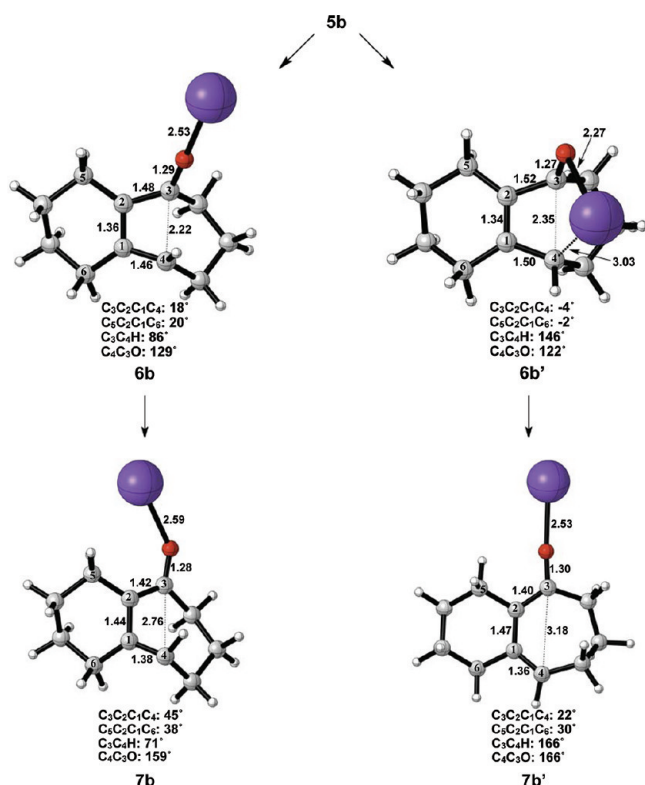


Figure 9. Optimized geometries of conrotatory (left) and non-pericyclic (right) ring-opening of cyclobutene potassium alkoxide **5b**. B3LYP/6-31G(d) selected bond distances (Å), angles, and dihedral angles are shown. LANL2DZ was used for potassium.

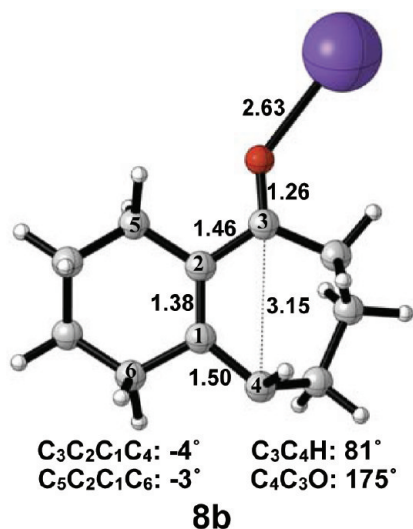


Figure 10. Optimized transition structure of isomerization of potassium alkoxide intermediate **7b** to **7b'**. B3LYP/6-31G(d) selected bond distances (Å), angles, and dihedral angles are shown.

C₃C₄H bond angle has only increased by 10° relative to **7b**. The activation enthalpy of *cis*–*trans* isomerization was calculated as 14 kcal/mol.

A better model for the experimental reaction conditions would be a fully THF-solvated potassium enolate, but this would be computationally highly challenging. The results are expected to be somewhere between the results for the potassium-coordinated and free anions.

Ring-Opening of the Cyclobutene Alcohol. We have also explored the extreme of coordination to the cyclobutene alkoxide, namely the corresponding alcohol. These results provide an assessment of allowed vs forbidden processes on a more conventionally substituted cyclobutene. Stationary points on the energy surface of electrocyclic ring-opening computed with B3LYP/6-31G(d) are shown in Figure 11. Thermally

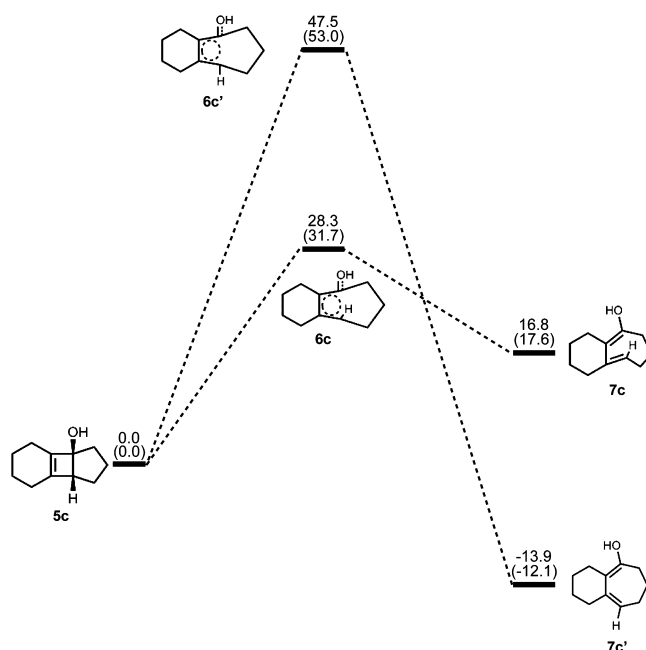


Figure 11. Stationary points on the energy surface for electrocyclic ring-opening. B3LYP/6-31G(d) thermal energies, ΔH , with thermally corrected M06–2X/6-311++G(d,p)//B3LYP/6-31G(d) energies, ΔH , in parentheses, shown in kcal/mol.

corrected M06–2X/B3LYP-6311++G(d,p) single point energies on B3LYP/6-31G(d) geometries are shown in parentheses. There is a preference of 19–21 kcal/mol for the allowed conrotatory ring-opening of the cyclobutenol, in spite of the 30 kcal/mol energetic preference for the less strained product that would result from forbidden disrotatory opening. This indicates that the normal preference for the allowed pathway is operating, in spite of large thermodynamic differences in the reactions.

The optimized geometries of conrotatory and disrotatory ring-opening of cyclobutenol are shown in Figure 12. The C₃–C₄ bond length of 1.60 Å in **5c** is unusually long but less stretched than the corresponding alkoxide. The bond angles and dihedral angles in the ring-opening transition structures are not appreciably different from those in the previous cases, but the three C–C bond lengths in the ring are nearly identical, showing significant delocalization that was not observed in the other cases. Conrotatory electrocyclic ring-opening is endothermic by 17–18 kcal/mol, while disrotatory ring-opening is exothermic by 12–14 kcal/mol. A summary of computed enthalpies for the model reaction including all basis sets and solvent models used is shown in Table 1. An analogous table reporting Gibbs free energies is given in the Supporting Information (Table S1).

Ring-Opening of an Alkoxide-Substituted Guanacastepene Precursor. Next, we expanded the investigation of ring-opening energetics to more complex systems incorporated

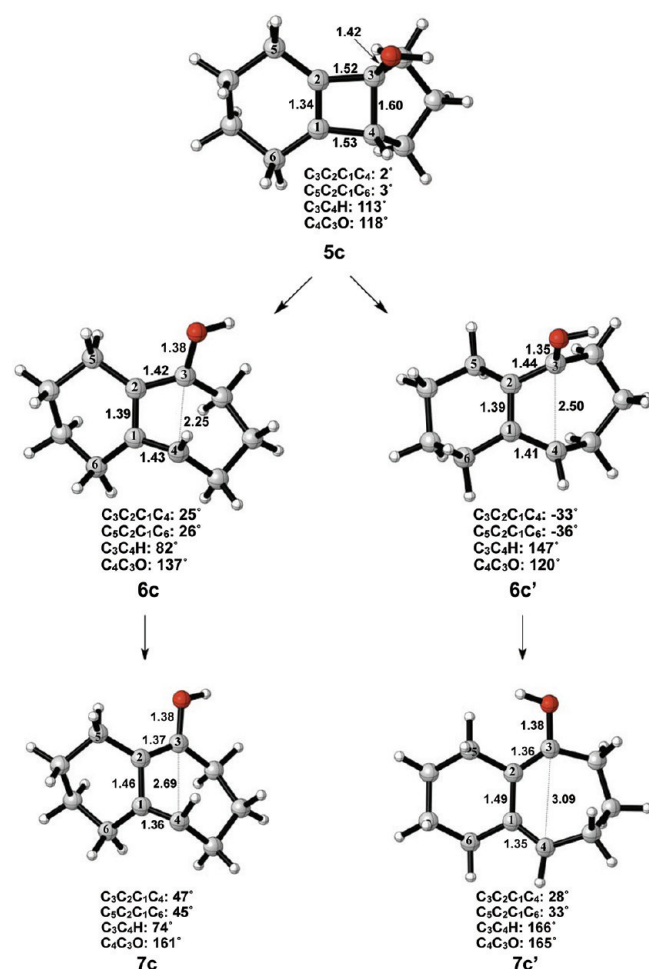


Figure 12. Optimized geometries of conrotatory (left) and disrotatory (right) ring-opening of cyclobutene alcohol **5c**. B3LYP/6-31G(d) selected bond distances (Å), angles, and dihedral angles are shown.

by Carreira.³ The electrocyclic ring-opening of anion **5d** was shown to favor the allowed conrotatory process; however, the observed preference of less than 1 kcal/mol is essentially negligible when considering error in B3LYP/6-31G(d) calculations. The thermally corrected M06-2X/6-311++G(d,p)//B3LYP/6-31G(d) single point energies show the energy gap to be 2 kcal/mol. Conrotatory product **7d** is less stable than cyclobutene enolate **5d** by 1 kcal/mol, while disrotatory product **7d'** is more stable than **5d** by 32 kcal/mol. The energetics of ring-opening are shown in Figure 13.

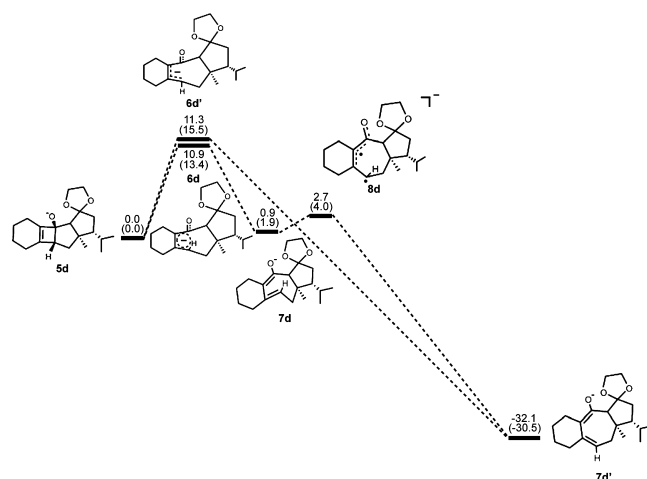


Figure 13. Stationary points on the energy surface for electrocyclic ring-opening of **5d**. B3LYP/6-31G(d) thermal energies, ΔH , with thermally corrected M06-2X/6-311++G(d,p)//B3LYP/6-31G(d) energies, ΔH , in parentheses, shown in kcal/mol.

Optimized geometries of conrotatory and nonpericyclic ring-opening are shown in Figure 14. The C_3C_4 bond length in **5d** is 1.68 Å, shorter than the 1.73 Å distance seen in the B3LYP/6-31G(d) optimized structure of cyclobutene enolate **5a**. This difference can be attributed to a decrease in donation of the C_3 -O nonbonding orbital into the C_3C_4 σ^* orbital due to electrostatic interactions of the alkoxide with hydrogens on an adjacent ring (**5d**, Figure 14), an effect qualitatively similar to coordination of the alkoxide with K^+ . This interaction is observed throughout the process of ring-opening. The C_3C_4 distances are very similar in the two transition structures **6d** and **6d'**, 2.39 and 2.43 Å respectively, unlike those seen when comparing the allowed and forbidden transition structures **6a-c** and **6a'-c'**. The $C_3C_2C_1C_4$ dihedral angles of **6d** and **6d'** are -17° and 13° , respectively. As mentioned previously, the disrotatory ring-opening transition structure of cyclobutene is planar,²⁵ so an observed dihedral angle of 13° in **6d'** is indicative of nonpericyclic character. Interestingly, the positive dihedral angles in **6d'** become negative in **7d'** (Figure 15). As a result, the carbon adjacent to C_4 in the cycloheptadiene ring has flipped from the concave to the convex side of the molecule.

Ring-Opening of a Potassium Alkoxide-Substituted Guanacastepene Precursor. The thermally allowed conrotatory electrocyclic ring-opening of potassium alkoxide **5e**

Table 1. Summary of Computed Enthalpies, ΔH , for the Model Alkoxide, Potassium Alkoxide, and Alcohol Systems

	gas phase			THF			
	a			c	b		
	B3LYP/6-31G(d)	B3LYP/6-311++G(d,p)	M06-2X	B3LYP/6-31G(d)	B3LYP/6-31G(d)	B3LYP/6-311++G(d,p)	B3LYP/6-31G(d)
1 + 2	0.0	0.0	0.0		0.0		0.0
3	-43.6	-35.9	-46.2		-33.8		-39.9
4	-41.8	-34.2	-41.3		-31.2		-36.9
5	-48.0	-41.6	-52.6	0.0	-41.5	0.0	-48.3
6	-45.5	-36.8	-46.6	28.3	-36.9	14.4	-33.7
6'	-44.4	-36.1	-43.8	47.5	-35.9	16.2	-33.0
7	-58.4	-49.6	-51.5	16.8	-48.5	3.1	-40.6
7'	-85.7	-75.3	-85.7	-13.9	-75.5	-22.5	-72.5
8	-44.0	-37.8	-47.7				-26.5

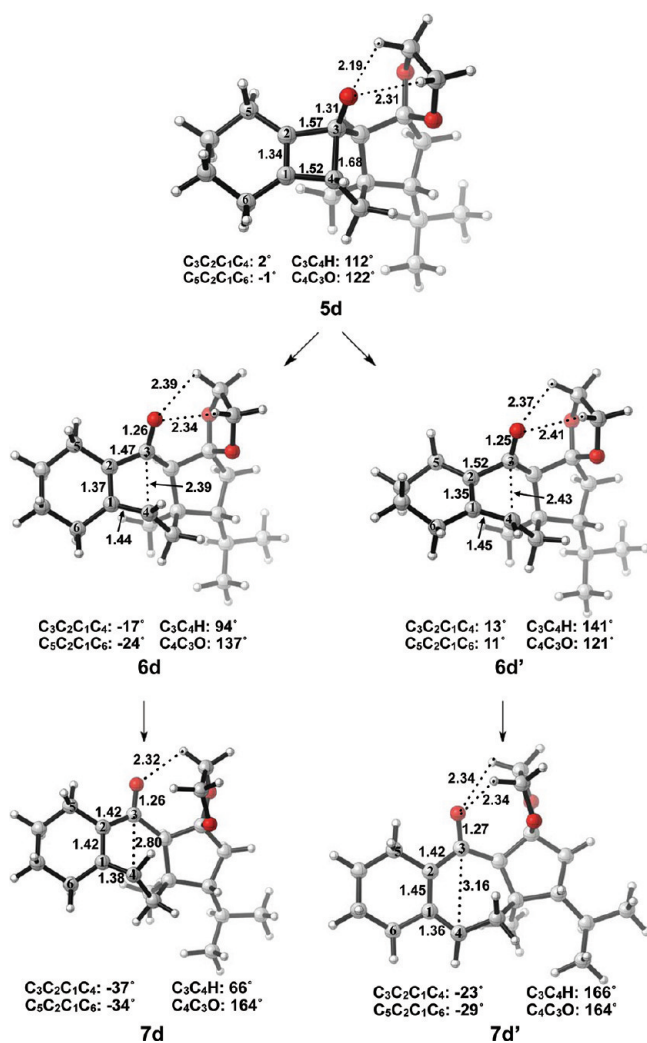


Figure 14. Optimized geometries of conrotatory (left) and nonpericyclic (right) ring-opening of 5d. B3LYP/6-31G(d) selected bond distances (Å), angles, and dihedral angles are shown.

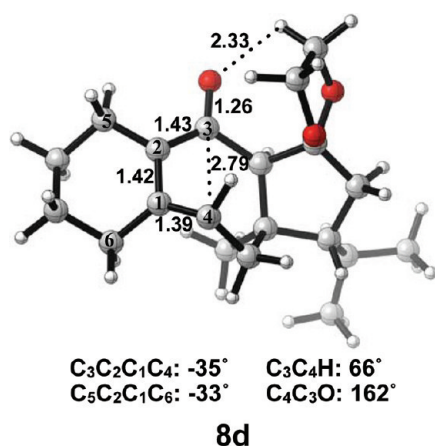


Figure 15. Optimized transition structure of isomerization of alkoxide intermediate 7d to 7d'. B3LYP/6-31G(d) selected bond distances (Å), angles, and dihedral angles are shown.

was disfavored by 8 kcal/mol, in sharp contrast to all other systems studied. Conrotatory product 7e is less stable than 5e by 9 kcal/mol, while 7e' is more stable than 5e by 22 kcal/mol.

Stationary points detailing the energetics of ring-opening of 5e are presented in Figure 16.

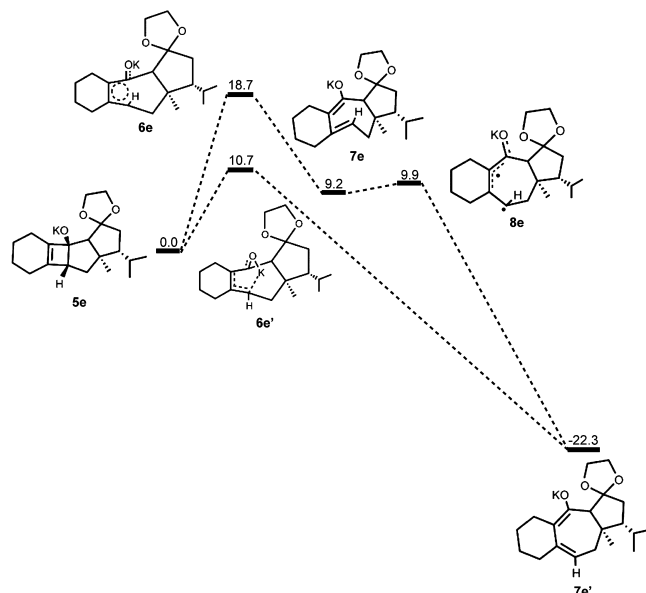


Figure 16. Stationary points on the energy surface for electrocyclic ring-opening of 5e. B3LYP/6-31G(d) thermal energies, ΔH , shown in kcal/mol.

Optimized geometries of conrotatory and nonpericyclic ring-opening are shown in Figure 17. The transition structure of isomerization from 7e to 7e' is shown in Figure 18. All relevant geometrical information is presented with the same interpretations as provided before; however, there is one important difference. In this molecule, there are other oxygen atoms to which the potassium atom can coordinate. Specifically in 6e', the coordination of the potassium to C4 and to another oxygen is likely responsible for the stabilization of this transition structure relative to 6e. With that idea in mind, a slight modification was made to replace the two oxygens in the adjacent ring with methylene carbons to form 5f. Ring-opening structures are shown in Figure 19, while Table 2 summarizes the ring-opening energies of 5d–f. Although replacing the oxygens in the ring with methylene groups did lower the energy difference between 6f and 6f' relative to 6e and 6e', Table 2 indicates a preference of 4 kcal/mol still remains for nonpericyclic ring-opening over conrotatory electrocyclic ring-opening. See Table S2 in the Supporting Information for Gibbs free energies.

ChelpG Calculations on the Mechanism of Ring-Opening. ChelpG (charges from electrostatic potentials using a grid-based method)²⁸ calculations on B3LYP/6-31G(d) optimized geometries were used to characterize the electronic structure of all ring-opening systems. Unlike the conrotatory transition structure of cyclobutene, the conrotatory transition structures 6a–f possess unequal charge distribution throughout the ring because of electronic effects originating from the oxygen on C3. The magnitude of negative charge on the oxygens in the nonpericyclic transition structures is close to that in the intermediates. This is uncharacteristic of electronic structure changes in pericyclic reactions, in which atomic charges gradually change throughout ring-opening. C4 develops a full negative charge in the anionic systems, decreasing from -0.1 in alkoxide 5 to -1.1 in transition state 6'. In the

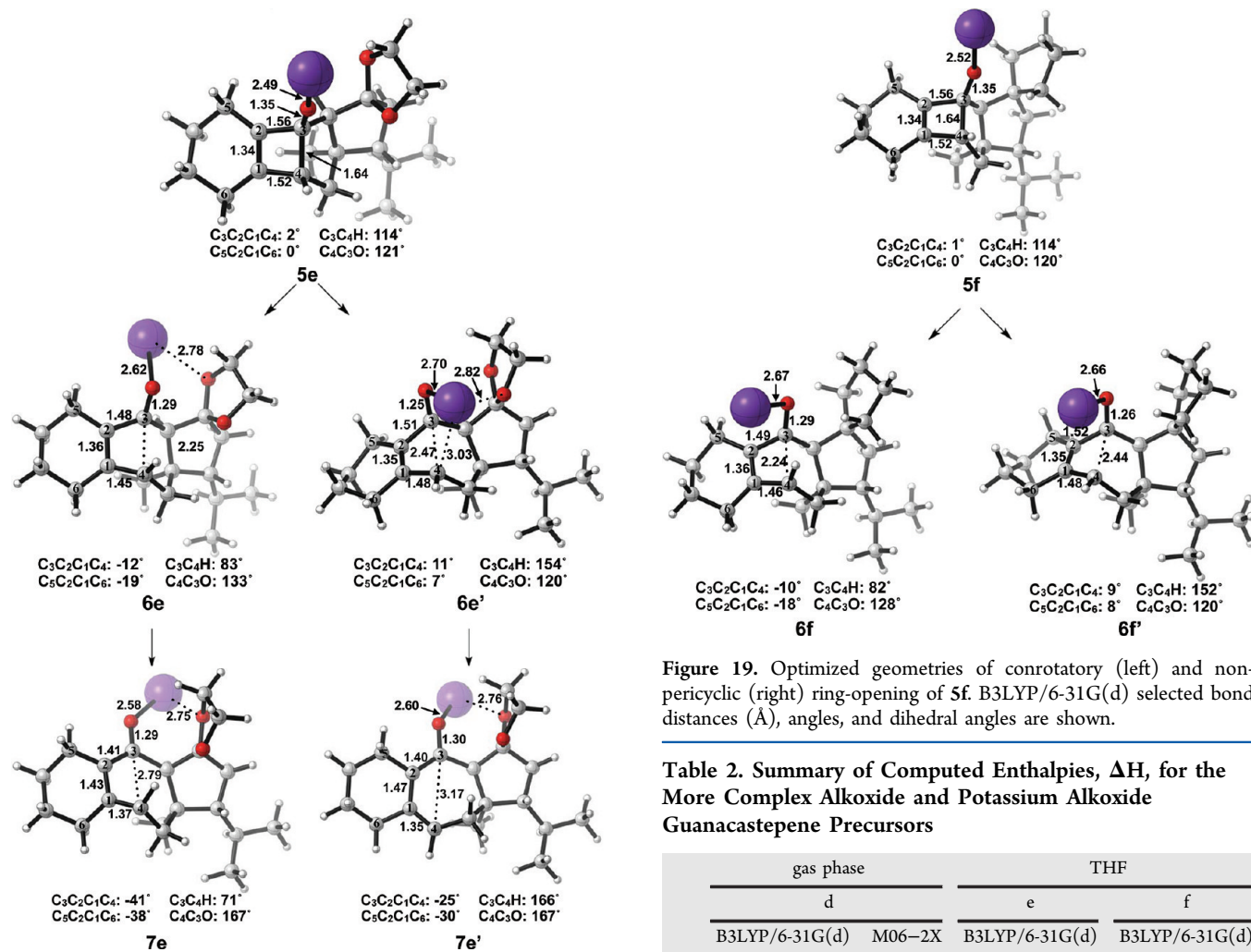


Figure 17. Optimized geometries of conrotatory (left) and non-pericyclic (right) ring-opening of 5e. B3LYP/6-31G(d) selected bond distances (Å), angles, and dihedral angles are shown.

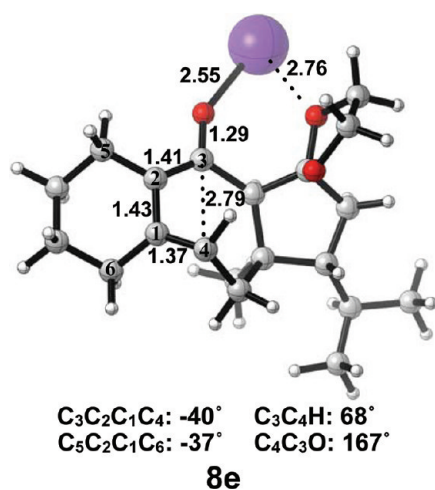


Figure 18. Optimized transition structure of isomerization of potassium alkoxide intermediate 7e to 7e'. B3LYP/6-31G(d) selected bond distances (Å), angles, and dihedral angles are shown.

potassium alkoxide systems, this charge buildup on C4 is stabilized by coordination of the potassium cation. Together, the trends in electronic structure of oxygen and C4 through

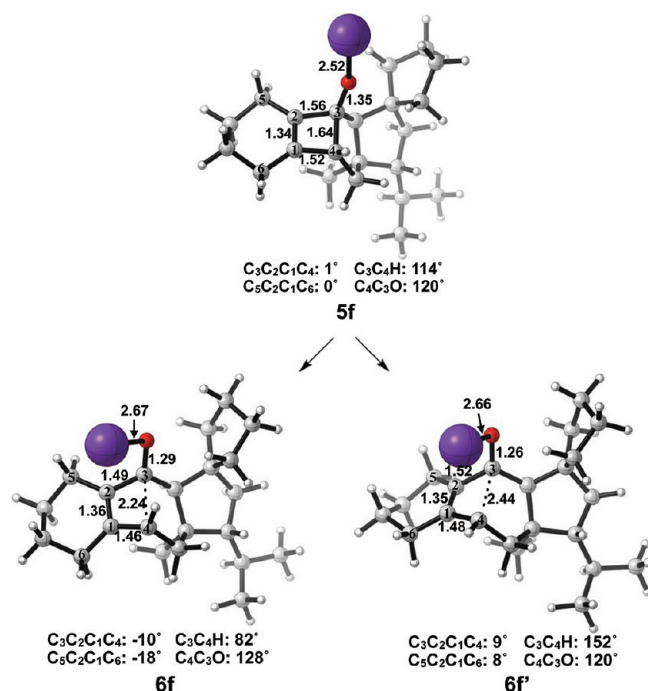


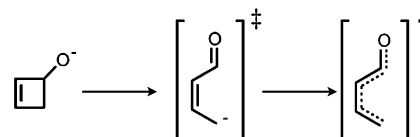
Figure 19. Optimized geometries of conrotatory (left) and non-pericyclic (right) ring-opening of 5f. B3LYP/6-31G(d) selected bond distances (Å), angles, and dihedral angles are shown.

Table 2. Summary of Computed Enthalpies, ΔH , for the More Complex Alkoxide and Potassium Alkoxide Guanacastepene Precursors

	gas phase		THF	
	d		e	f
	B3LYP/6-31G(d)	M06-2X	B3LYP/6-31G(d)	B3LYP/6-31G(d)
5	0.0	0.0	0.0	0.0
6	10.9	13.4	18.7	17.4
6'	11.3	15.5	10.7	13.7
7	0.9	1.9	9.2	
7'	-32.1	-30.5	-22.3	
8	2.7	4.0	9.9	

5–6'–7' provide evidence against a pericyclic disrotatory ring-opening. Instead, the mechanism resembles carbonyl formation in the transition state with anion migration to C4 upon C–C bond cleavage (Scheme 4). Ring-opening of 5c is the only

Scheme 4. Schematic Representation of Nonpericyclic Ring-Opening



system that displays true forbidden disrotatory nature, as shown by the magnitude of difference in energies between the two pathways and the plots of atomic charges. Figure 20 shows the atomic charges of the four carbons in the cyclobutene ring and of the oxygen on C3 throughout both ring-opening pathways of 5a. Corresponding plots of all systems presented in this paper

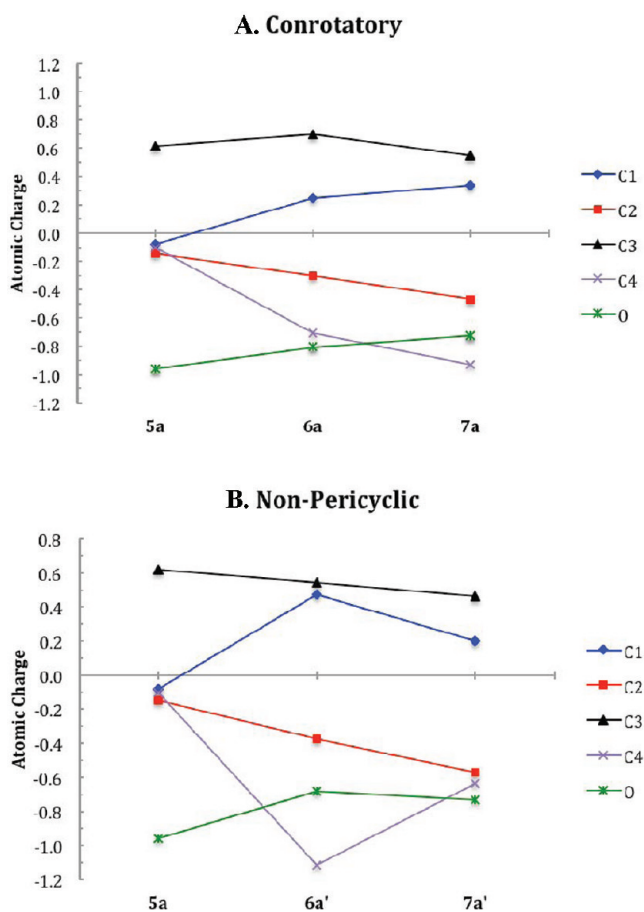


Figure 20. Atomic charges on the four carbons and the oxygen substituent in the cyclobutene ring of 5a through (A) the conrotatory electrocyclic ring-opening and (B) the nonpericyclic ring-opening.

and numerical tables of charges are given in the Supporting Information.

CONCLUSIONS

The large preference for allowed conrotatory ring-opening in the cyclobutene alcohol becomes very small in the alkoxide, presumably because of the very early transition states arising from the very large exothermicity of the reaction. The C₁–C₄ and C₂–C₃ bonds in 6a, 6a', 6b, and 6b' show primarily single bond character (1.46–1.52 Å), which, along with the fact that the C₁–C₂ bonds are 1.34–1.36 Å, indicates a very early transition state.

In the gas phase reaction of the free alkoxide, the mechanism is a conrotatory electrocyclic ring-opening pathway that is preferred by 1–3 kcal/mol, followed by *cis*–*trans* isomerization with a barrier of 6–12 kcal/mol to give the experimentally observed product (Figure 3). In the reaction model where oxygen is coordinated with potassium in THF, as seen in Figure 8, conrotatory ring-opening is also preferred by about 1 kcal/mol; however, *cis*–*trans* isomerization is unfeasible at low temperatures, as this barrier is 7 kcal/mol higher than the barrier for electrocyclic ring closing. This suggests a mechanism in which there is equilibration of conrotatory ring-opening and closing with a percentage of nonpericyclic ring-opening to give the thermodynamic product. In the gas phase reaction of the free alkoxide 5d, the mechanism is an allowed conrotatory ring-opening followed by *cis*–*trans* isomerization to give 7d'. For the

ring-openings of potassium alkoxides 5e and 5f in THF, the mechanism follows a nonpericyclic ring-opening that is 8 and 4 kcal/mol lower than conrotatory ring-opening, respectively. This appears to be the mechanism studied by the Carreira group. ChelpG calculations of the ring-opening pathways help show that the forbidden “disrotatory” mechanism is, in fact, nonpericyclic in nature.

ASSOCIATED CONTENT

Supporting Information

Cartesian coordinates, computed total energies of all optimized structures, imaginary frequencies of all transition structures, and plots of ChelpG atomic charges. This material is available free of charge via the Internet at <http://pubs.acs.org>.

AUTHOR INFORMATION

Corresponding Author

*E-mail: houk@chem.ucla.edu.

Notes

The authors declare no competing financial interest.

ACKNOWLEDGMENTS

We are grateful to the National Institutes of Health for financial support (R01 GM036700) and to Erick M. Carreira for helpful discussions.

REFERENCES

- (1) Tambar, U. K.; Stoltz, B. M. *J. Am. Chem. Soc.* **2005**, *127*, 5340–5341.
- (2) Gampe, C. M.; Boulos, S.; Carreira, E. M. *Angew. Chem., Int. Ed.* **2010**, *49*, 4092–4095.
- (3) Gampe, C. M.; Carreira, E. M. *Angew. Chem., Int. Ed.* **2011**, *50*, 2962–2965.
- (4) Gampe, C. M.; Carreira, E. M. *Angew. Chem., Int. Ed.* **2012**, *51*, 3766–3778.
- (5) Comandini, A.; Brezinsky, K. *J. Phys. Chem. A* **2012**, *116*, 1183–1190.
- (6) Frisch, M. J.; et al. *Gaussian 09*, revision A.02; Gaussian, Inc.: Wallingford, CT, 2009.
- (7) Staroverov, V. N.; Davidson, E. R. *J. Am. Chem. Soc.* **2000**, *122*, 7377–7385.
- (8) Pieniazek, S. N.; Clemente, F. R.; Houk, K. N. *Angew. Chem., Int. Ed.* **2008**, *47*, 7746–7749.
- (9) Fukui, K. *J. Phys. Chem.* **1970**, *74*, 4161–4163.
- (10) Deng, L.; Ziegler, T. *Int. J. Quantum Chem.* **1994**, *52*, 731–765.
- (11) Barone, V.; Cossi, M. *J. Phys. Chem. A* **1998**, *102*, 1995–2001.
- (12) Takano, Y.; Houk, K. N. *J. Chem. Theory Comput.* **2005**, *1*, 70–77.
- (13) Cheong, P. H.-Y.; Paton, R. S.; Bronner, S. M.; Im, G.-Y. J.; Garg, N. K.; Houk, K. N. *J. Am. Chem. Soc.* **2010**, *132*, 1267–1269.
- (14) Olivella, S.; Pericàs, M. A.; Riera, A.; Solé, A. *J. Org. Chem.* **1987**, *52*, 4160–4163.
- (15) Johnson, R. P.; Daoust, K. J. *J. Am. Chem. Soc.* **1995**, *117*, 362–367.
- (16) Yavari, I.; Nasiri, F.; Djahaniani, H.; Jabbari, A. *Int. J. Quantum Chem.* **2005**, *106*, 697–703.
- (17) Rondan, N. G.; Houk, K. N. *J. Am. Chem. Soc.* **1985**, *107*, 2111–2121.
- (18) Cooper, W.; Walters, W. D. *J. Am. Chem. Soc.* **1958**, *80*, 4220–4224.
- (19) Dolbier, W. R., Jr.; Koroniak, H.; Houk, K. N.; Sheu, C. *Acc. Chem. Res.* **1996**, *29*, 471–477.
- (20) Breulet, J.; Schaefer, H. F., III. *J. Am. Chem. Soc.* **1984**, *106*, 1221–1226.
- (21) Brauman, J. I.; Golden, D. M. *J. Am. Chem. Soc.* **1968**, *90*, 1920–1921.

- (22) Ross, J. A.; Seiders, R. P.; Lemal, D. M. *J. Am. Chem. Soc.* **1976**, *98*, 4325–4327.
- (23) Fabian, W. M. F.; Bakulev, V. A.; Kappe, C. O. *J. Org. Chem.* **1998**, *63*, 5801–5805.
- (24) Ji, H.; Li, L.; Xu, X.; Ham, S.; Hammad, L. A.; Birney, D. M. *J. Am. Chem. Soc.* **2009**, *131*, 528–537.
- (25) Lee, P. S.; Sakai, S.; Hörstermann, P.; Roth, W. R.; Kallel, E. A.; Houk, K. N. *J. Am. Chem. Soc.* **2003**, *125*, 5839–5848.
- (26) López, C. S.; Faza, O. N.; de Lera, A. R. *Chem.—Eur. J.* **2007**, *13*, 5009–5017.
- (27) Qin, C.; Davis, S. R. *J. Org. Chem.* **2003**, *68*, 9081–9087.
- (28) Johnson, r. P.; Daoust, K. J. *J. Am. Chem. Soc.* **1996**, *118*, 7381–7385.
- (29) Inoue, Y.; Hagiwara, S.; Daino, Y.; Hakushi, T. *J. Chem. Soc., Chem. Commun.* **1985**, *19*, 1307–1309.